

Clark Miles (Orcid ID: 0000-0001-7058-8776)

Bennett Georgina (Orcid ID: 0000-0002-4812-8180)

## **Untangling the controls on bedload transport in a wood-loaded river with RFID tracers and linear mixed modelling**

Miles J. Clark<sup>1</sup>, Georgina L. Bennett<sup>2</sup>, Sandra E. Ryan-Burkett<sup>3</sup>, David A. Sear<sup>4</sup> and Aldina M. A. Franco<sup>1</sup>

<sup>1</sup>School of Environmental Science, University of East Anglia, Norwich, United Kingdom

<sup>2</sup>Department of Geography, University of Exeter, Exeter, United Kingdom

<sup>3</sup>Forest Service, Rocky Mountain Research Station, Fort Collins, United States

<sup>4</sup>University of Southampton, Southampton, United Kingdom of Great Britain

### **Corresponding Author**

Miles Clark

School of Environmental Sciences,  
University of East Anglia, Norwich Research Park,  
Norwich, NR4 7TJ, United Kingdom

Tel: 07933612127

Email: [m.clark@uea.ac.uk](mailto:m.clark@uea.ac.uk)

### **Co-author Details**

Georgina L Bennett - [g.l.bennett@exeter.ac.uk](mailto:g.l.bennett@exeter.ac.uk)

Aldina M. A. Franco - [A.Franco@uea.ac.uk](mailto:A.Franco@uea.ac.uk)

Sandra E. Ryan-Burkett - [sandra.e.ryan-burkett@usda.gov](mailto:sandra.e.ryan-burkett@usda.gov)

David A. Sear - [D.Sear@soton.ac.uk](mailto:D.Sear@soton.ac.uk)

### **Acknowledgments**

This article has been accepted for publication and undergone full peer review but has not been through the copyediting, typesetting, pagination and proofreading process which may lead to differences between this version and the Version of Record. Please cite this article as doi: 10.1002/esp.5376

Banning Starr and Doug McClain at USFS Fraser experimental headquarters helped to accommodate us and offer logistical support while on field work, in addition to technical assistance with electronic equipment. Additionally, Sara Rathburn provided intermediate accommodation while traveling to field site.

### **Financial Support**

This research has been funded by UKRI via the Natural Environment Research Council and Engineering and Physical Sciences Research Council through the NEXUSS DTP.

### **Author Contributions**

**Miles Clark:** Conceptualization, Investigation, Formal analysis, Writing - Original Draft

**Georgina Bennett:** Supervision, Conceptualization, Writing - Review & Editing,

Investigation **Sandra Ryan-Burkett:** Investigation, Writing - Review & Editing **David**

**Sear:** Writing - Review & Editing **Aldina Franco:** Supervision, Writing - Review & Editing

### **Data availability statement**

The authors confirm that the data supporting the findings of this study are available within the article. Raw data that support the findings of this study are available from the corresponding author, upon reasonable request.

### **Conflict of Interest Statement:**

The authors have no conflicts of interest to declare. There is no financial interest to report.

We certify that the submission is original work and is not under review at any other publication.

## Reference Additions

Arnaud, F., Piégay, H., Vaudor, L., Bultingaire, L. and Fantino, G., 2015. Technical specifications of low-frequency radio identification bedload tracking from field experiments: Differences in antennas, tags and operators. *Geomorphology*, 238, 37-46.

Bates, D., Mächler, M., Bolker, B., & Walker, S. (2015). Fitting Linear Mixed-Effects Models Using lme4. *Journal of Statistical Software*, 67(1).

Cassel, M., Piégay, H., Fantino, G., Lejot, J., Bultingaire, L., Michel, K., Perret, F. (2020) Comparison of ground-based and UAV a-UHF artificial tracer mobility monitoring methods on a braided river, *Earth Surface Processes and Landforms*, 45, 1123 – 1140.

Chapuis, M., Bright, C.J., Hufnagel, J. and MacVicar, B., 2014. Detection ranges and uncertainty of passive Radio Frequency Identification (RFID) transponders for sediment tracking in gravel rivers and coastal environments. *Earth Surface Processes and Landforms*, 39(15), 2109-2120.

Ferguson, R.I., (2005). Estimating critical stream power for bedload transport calculations in gravel-bed rivers. *Geomorphology*, 70(1-2), 33-41.

Hassan, M. A. and D. N. Bradley (2017). Geomorphic controls on tracer particle dispersion in gravel-bed rivers. *Gravel-Bed Rivers: Process and Disasters*: 159-184.

Lamarre, H., MacVicar, B. and Roy, A.G., 2005. Using passive integrated transponder (PIT) tags to investigate sediment transport in gravel-bed rivers. *Journal of Sedimentary Research*, 75(4), 736-741.

MacVicar, B. J. and Papangelakis, E., (2022) Lost and found: Maximizing the information from a series of bedload tracer surveys. *Earth Surface Processes and Landforms*, 47(2), 399-408.

McDermott Long, O., Warren, R., Price, J., Brereton, T.M., Botham, M.S. and Franco, A.M., (2017) Sensitivity of UK butterflies to local climatic extremes: which life stages are most at risk?. *Journal of Animal Ecology*, 86(1), 108-116.

Nichols, M. H., (2004) A radio frequency identification system for monitoring coarse sediment particle displacement. *Applied Engineering Agriculture* 20, 783–787.

Petit, F., Gob, F., Houbrechts, G. and Assani, A.A., 2005. Critical specific stream power in gravel-bed rivers. *Geomorphology*, 69(1-4), 92-101.

Pyrce, R. S. and P. E. Ashmore (2003). "Particle path length distributions in meandering gravel-bed streams: Results from physical models." *Earth Surface Processes and Landforms* 28(9): 951-966.

Steeb, N., Rickenmann, D., Badoux, A., Rickli, C. and Waldner, P., 2017. Large wood recruitment processes and transported volumes in Swiss mountain streams during the extreme flood of August 2005. *Geomorphology*, 279, 112-127.

*References were included upon the suggestion of both reviewers, in addition to providing background information on further analysis undertaken to appropriately respond to reviewers' comments.*

## **Abstract**

Bedload transport is a fundamental process by which coarse sediment is transferred through landscapes by river networks and may be well described stochastically by distributions of grain step length and rest time obtained through tracer studies. To date, none of these published tracer studies have specifically investigated the influence of large wood in the river channel on sediment transport dynamics, limiting the applicability of stochastic sediment transport models in these settings. Large wood is a major component of many forested rivers and is increasing due to anthropogenic 'Natural Flood Management' (NFM) practices. This study aims to investigate and model the influence of large wood on grain-scale bedload transport.

We tagged 957 cobble – pebble sized particles ( $D_{50} = 73$  mm) and 28 pieces of large wood (> 1 m in length) with RFID tracers in an alpine mountain stream. We monitored the transport distance of tracers annually over three years, building distributions of tracer transport distances with which to compare with published distributions from wood free settings. We also applied linear mixed modelling (LMM), to tease out the influence of wood from other controls on likelihood of entrainment, deposition, and the transport distances of sediments.

Tracer sediments accumulated both up and downstream of large wood pieces, with LMM analysis confirming a reduction in the probability of entrainment of tracers closer to wood in all three years. Upon remobilisation, tracers entrained from positions closer to large wood had shorter subsequent transport distances in each year. In 2019, large wood also had a trapping effect, significantly reducing the transport distances of tracer particles entrained from upstream, i.e. forcing premature deposition of tracers. This study demonstrates the role of large wood in influencing bedload transport in alpine stream environments, with implications for both natural and anthropogenic addition of wood debris in fluvial environments.

**Key Words:** Bedload transport, large wood, tracers, RFID, linear mixed modelling

## 1. Introduction

Large wood (defined as pieces  $> 1$  m length and 0.1 m diameter, Wohl *et al.* 2010), is a major component of many forested rivers and can increase following disturbances such as wildfire (Bendix and Cowell, 2010), insect infestations (Ryan *et al.*, 2012), mass movements, bank erosion (Steeb *et al.*, 2017), and the anthropogenic addition of wood as part of Natural Flood Management (NFM) (Grabowski *et al.*, 2019). The latter has seen an increase in popularity to help regulate flow regimes, alter sediment dynamics, and support habitats (e.g., Gippel *et al.*, 1996; Klaar *et al.*, 2011; Langford *et al.*, 2012; Dixon & Sear, 2017; Dadson *et al.*, 2017). The presence of wood in a fluvial system has a major influence on sediment storage with Gregory *et al.* (1994) and Wohl and Scott (2017) finding a greater residual pool volume associated with increasing large wood loads. Large wood has also been observed to reduce overall sediment transport rates (Montgomery *et al.*, 2003), significantly altering the geomorphological characteristics of streams through the formation of log steps (Ryan *et al.*, 2014), in addition to strengthening channel-hillslope coupling (Golly *et al.*, 2019) and adding geomorphic complexity to streams. However, there has been a lack of research into the influence of large wood on stochastic grain-scale sediment transport, which is fundamental for understanding and modelling the dispersion of sediment pulses through the fluvial system. Pulses of sediment may enter fluvial systems through a range of anthropogenic processes, including mining (Pickup *et al.*, 1983; Ferguson *et al.*, 2015), dam removal (East *et al.*, 2015), and road runoff (Lane and Sheridan, 2002), in addition to natural processes, including logjam break up (Umazano and Melchor, 2020), landsliding (Sutherland *et al.*, 2002) and cyclic erosion of bedforms (Dhont and Ancely, 2018). These pulses have a range of impacts on the fluvial system as they disperse or translate downstream. They can cause changes in

channel capacity, with impacts on flood hazard (e.g., Slater *et al.*, 2015) and risk to people who live near or depend on fluvial environments. Furthermore, understanding both the dispersion of pulses of sediment and individual grain transport is essential for the progression of engineering approaches and fluvial research in a range of applications, including contaminant transportation (Reneau *et al.*, 2004; Malmon, 2005), fluvial sediment budgets (Kelsey, 1987; Malmon *et al.*, 2003) and restoration of rivers (Sear, 1994; Kinzel, 2009; Gaeuman *et al.*, 2017).

The dispersion of a pulse of sediment can be modelled using a stochastic approach in which bedload transport is described and modelled probabilistically, in recognition that bedload transport is characterized by cyclic sequences of particle motion and rest (e.g., Ancey, *et al.*, 2008; Lajeunesse, 2017). Individual grain transport was initially recognised to be intermittent and probabilistic by Einstein (1937), with the development of a probability function and a transport rate equation in which bedload transport occurs in a series of steps resulting from the turbulent fluctuations caused when hydrodynamic lift forces are greater than a particle's weight. Consequently, the transport of coarse-grained sediments is not continuous, with particles predominantly remaining at rest, even when fluid stress is above the threshold of movement.

Numerous tracer studies have characterised the stochastic behaviour of bedload transport by measuring distributions of grain step lengths and rest times of tracer particles (e.g., Bradley and Tucker, 2012; Ancey *et al.*, 2014; Olinde and Johnson, 2015; Ancey and Bohorquez, 2018). Different methodologies of tracers include the painting of rocks, radio transmitters, and the use of magnetic clasts (e.g., Keller, 1970, Laronne & Carson, 1976; Hassan *et al.*, 1991; Ferguson & Wathen, 1998). These methods have limitations including difficulties recognising individual clasts, loss of sediments due to burial, and anthropogenic interference. Tracer experiments have become progressively more sophisticated over the last 50 years,

with radio frequency identification (RFID) tracer technology becoming the most favoured technique (Sear *et al.*, 2003; Hassan & Ergenzinger, 2003; Cassel *et al.*, 2020; MacVicar & Papangelakis, 2022).

Previous studies evaluating bedload sediment transport and its dispersion characteristics with tracers of various kinds have found step length frequency distributions to most closely fit an exponential or gamma distribution (e.g., Habersack, 2001; McNamara and Borden, 2004; Bradley and Tucker, 2012), where the majority of particles have small step lengths and progressively fewer have longer displacement distances. Additionally, the diffusion of bedload sediments is determined by the tail character of the exceedance probability plots, and are typically seen to be heavy or thin, which is indicative of anomalous diffusion (e.g., Olinde and Johnson, 2015; Bradley, 2017). This type of diffusion is determined by the probability distributions of the step scaling, step lengths, and resting times. Where distributions, in combination, control the migration of particles, and the variance of displacement increases more rapidly or slowly with time than in non-linear diffusion and is therefore anomalous rather than Fickian (Martin *et al.*, 2012). This can be expressed by  $\sigma^2 \sim t^\gamma$ , with  $\gamma > 1$  and  $\gamma < 1$  representing superdiffusion and subdiffusion respectively (Weeks & Swinney, 1998). A detailed explanation of the dispersion characteristics of bedload is found within Nikora (2002), which covers particles in motion through sliding, rolling, and saltation but not total suspension.

In environments with high wood loading, the influence of large wood pieces on rock step lengths, rest times, and subsequent dispersion characteristics is currently unknown, limiting the applicability of stochastic sediment transport models in these settings. It is theorised that the presence of large wood increases bed surface roughness (e.g., Buffington and Montgomery, 1999), subsequently reducing the shear stress on the riverbed and subsequent sediment transport distances. Furthermore, geomorphic features formed due to woods



presence, such as scour pool structures, can increase particle burial rates (e.g., Wohl and Scott, 2017) in addition to wood physically blocking sediment movement.

In this study, we aimed to evaluate the impact of large wood on grain-scale stochastic bedload transport dynamics. We undertook a sediment tracer study at a wood-loaded reach using passive RFID tags embedded in individual clasts to quantify sediment transport distances, and investigate their distribution over a three-year period with respect to wood loading, allowing comparison with previous studies in wood-free fluvial settings (e.g., Bradley, 2017).

Additionally, we applied linear mixed modelling (LMM) to tease out the influence of wood on sediment transport dynamics from the myriad of other controls. This technique is commonly used in ecological and biological research to determine the controls on animal behaviour (e.g., McDermott-Long et al., 2017; Dunnink et al., 2019) and while this approach is novel in earth sciences, the principle of treating tracers as individuals within a larger population with varying but similar influencing variables is analogous to individual animals within a population of a species in ecological sciences. Specifically, we used LMM to untangle the influence of wood on the probability of tracer entrainment, deposition and transport distance, from other controls including tracer size and location relative to the thalweg, boulders and steps.

Our findings have implications for predicting bedload sediment transport and downstream deposition. Additionally, field data will assist in determining the effectiveness and potential side effects of introducing engineered log jams in river management schemes (Bennett *et al.*, 2015), as well as provide information for their installation. Finally, we demonstrate the

potential of the LMM technique for tracer studies attempting to untangle the multiple controls on bedload transport.

## 2. Study site

The study site is St. Louis Creek (figure 1), a gravel bed subalpine stream characterised primarily by a step pool morphology with small sections of pool riffle at the upstream segment of the investigated area. The bed grain size distributions are  $D_{16}$ ,  $D_{50}$ , and  $D_{84}$  of 30, 53, and 77 mm respectively. Steps are primarily formed from a combination of boulders and pieces of wood incorporated into the bed (figure 2). The area of the reach investigated is 220 m in length and has an average slope of 0.046. There are 4 log and 10 boulder steps present along the study area in addition to small patches of vegetation and gravel bars. The site is located within the Fraser Experimental Forest (FEF), Colorado. The FEF is located approximately 80 km northwest of Denver with an elevation above ~2700 m, and is an experimental area managed by the U.S. Forest Service. Its watershed is underlain mostly by granite, gneiss, and schist bedrock (Green, 1992).

St. Louis Creek is a second order stream, with a flow regime characterised by snowmelt runoff, with flow rates generally beginning to rise during April, typically peaking throughout May, June, and July and returning to base flow in late summer (figure 3). Because of this, the field season surveys took place during late summer, when water levels are low enough for particle relocation and the winter snows have yet to begin restricting access to the site.

The site is ideal for studying the influence of large wood on sediment transportation as it is undergoing an increase in wood loading due to the death of the majority of the old growth Lodgepole pine (*P. contorta*), resulting from infestations of the mountain pine beetle (*Dendroctonus ponderosae*) (Raffa *et al.*, 2008). The site therefore acts as a natural case

study for the impact of wood loading, its influence on geomorphic change, and sediment transport. Wood at the site is present in the form of log steps, ramps, bridges, and incorporated jams (Wohl *et al.*, 2010), with > 75 % of surveyed pieces attached or incorporated into the banks.

The study area is subdivided into two main reaches, distinguished by morphology and channel slope (figure 2b). Firstly, the “seeded” reach which covers the area of initial instillation of tracer sediments (figure 1b). It extends 35 m downstream streamwise, with channel widths ranging from 3 to 10 m (average 6.8 m) and has a slope of 0.0328.

Morphology here is less complex than further downstream, with small gravel bars and pool riffle sequences. The channel here is unconfined. Secondly, the “wooded” reach is downstream of the seeded reach and has significant wood loading. It extends 185 m downstream streamwise, with channel widths ranging from 3.2 to 9.7 m (average 5 m) and a slope of 0.0502. Morphology here is more complex with pools and steps formed from a combination of boulders and wood pieces (e.g., figure 1e) with downstream sections of the reach becoming confined.

### **3. Methods**

RFID is an wireless identification system with a variety of applications in environmental science (e.g., biotracking (Floyd, 2015), wood tracking (Schenk *et al.*, 2014), and sediment transport (Nichols, 2004; Lamarre *et al.*, 2005). It provides the ability to remotely identify individual items of interest, making it ideal for studying individual clasts during bedload transport. The technology relies primarily on two pieces of hardware: a passive integrated transponder (PIT tag), which is used to mark objects of interest, and a reader (or antenna) which acts as a transmitter and a receiver. This study used a long-range Oregon RFID mobile

reader kit (Oregon RFID, 2021), with 32 x 3.65 mm PIT tags weighing 0.8 g each, which can be embedded into clasts with a b-axis as small as 47 mm with minimal effect on shape and density of clasts. See Nichols (2004) for detailed description of RFID particle tracking methodology.

Initially, 957 cobble to pebble sized clasts were selected, due to their similarity in composition and size to bed materials, in addition to their suitability for tagging. Clast weight and axes size were recorded (table 1), and the selected clasts were drilled to allow space for the implanting of the passive RFID PIT tags. Once tags were inserted, silicone was used to seal the tags within the clasts, producing tracer sediments that appeared unchanged compared to the natural sediments of the study site. As a failsafe in case of tag failure, and initial identification of tracers, the corresponding RFID identification numbers were written on the surface of tagged clasts.

In addition to sediments, pieces of large wood (typically trunks from adjacent riparian areas) were tagged and measured, and an inventory of their defining characteristics, including length, diameter and structural associations, was collected based on agreed definitions (Wohl *et al.*, 2010) and are available in supplementary information (S1). While many pieces of large wood classified as bridges were characterised and tagged, they were not included in subsequent sediment transport analysis due to their current lack of interaction with the bed, even during high flow. Finally, a discharge gauge was installed at the upstream end of the study site, which collected flow data from May to October from 2017 – 2019. There are no substantial tributaries located along the study reach, therefore flow rates characterize the whole site. Flow rates recorded in St. Louis Creek (figure 3) match well with another gaged river, Bobtail Creek (figure 4), whose record extends from 1986 – 2019, facilitating estimation of the recurrence interval of transporting flows within the study stream, assuming the flows have always been analogous due to proximity, similar forest cover, aspect and

altitude of sites. We calculated related stream power using surveyed slope, channel width, and discharge (Petit et al., 2005).

Tracer clasts were seeded in summer 2016, in a 0.5 m grid across the channel from bank to bank. This channel segment is referred to as the “seeded” reach (figure 1b) that extended from the location of the discharge gauge to ~ 35 m downstream. Deployment of tracers was on the surface of the bed, resulting in tracers beginning in highly mobile positions (e.g., Bradley and Tucker, 2012), analogous to the most mobile surface grains of the pre-existing bed surface. Spatial locations of tracer sediments were recorded using a Leica total station with a known GPS location and a reflector placed above tracer sediment locations. It has been established that both clustering and orientation of transponders can add uncertainty to detection ranges (*Chapuis et al.*, 2014; *Arnaud et al.*, 2015). However, we conducted burial experiments of the tagged clasts and established that tracer IDs could be read from ~ 0.70 m, with minimum interference from water or surrounding and overlying sediments.

Tracer sediments and wood locations were resurveyed on an annual basis after annual snowmelt in 2017, 2018 and 2019 using an Oregon RFID mobile reader setup which included a backpack, antenna, and mobile reader. Tracers were considered mobile, and their new deposition location recorded if transport was > 1 m to account for the potential variation in detection distances each year. Wood debris was classified as significant and surveyed if it is at least 10 cm in diameter and > 1 m in length following the parameters suggested by Wohl *et al.* (2010). Additional characteristics such as size, classification (e.g., ramp or bridge type), and state of decay was recorded annually to determine if these characteristics impacted interaction with sediment transport or subsequent wood transport (e.g., Dixon & Sear, 2016). Additionally, other geomorphic features within the study site were surveyed, such as the location of banks, steps, and boulders. All spatial data was recorded in ArcGIS10, alongside supplementary information (e.g., size or defining characteristics of wood pieces) producing a

spatially accurate map of the area which was updated every year (e.g., figure 1a). Annual spatial locations of tracers are available in supplementary information (S2).

To produce accurate tracer transport data, cartesian GPS locations of tracers were converted into a channel-based coordinate system, as the spatial referencing of river channels is complicated by meandering. Coordinates were converted following the methods of Legleiter & Kyriakidis (2006), which consider the channel centre line as the streamwise axis (i.e. relative distance downstream), allowing travel distances to be corrected for channel curvature.

Annually resurveying tracer locations after high flow conditions during snowmelt resulted in a dataset spanning 3 years of tracer transport distances, which we were able to use to investigate and evaluate any disruption to “typical” transport behaviour introduced by the presence of large wood.

### **3.2 Statistical analysis and modelling**

Quantifying and modelling rock-step length and rest time distributions allows accurate predictions to be made of bedload transport in fluvial environments using established statistical estimation methods of previous tracer studies (e.g., Hassan, *et al.*, 2013; Olinde and Johnson, 2015). The length of our study of 3 years precluded analysis of particle rest time but we are able to plot meaningful tracer transport distance distributions for comparison with published studies in wood-free settings. Exponential and gamma distributions were fitted to the tracer transport distance frequency data (figure 5). In order to identify the likely type of sediment diffusion (super or sub diffusive), we quantified the exponent on the tail of the exceedance probability distribution of tracer transport distances. This was conducted in MATLAB (R2018B) by fitting a power-law distribution model to the tail of the distribution

following the methods of Clauset *et al.* (2009), where  $x_{\min}$  for 2017, 2018, and 2019 was calculated to be 33.45, 5.77, and 41.06 respectively.

Linear mixed modelling was used for determining the influence that individual variables (e.g., proximity to large wood) have, on a continuous dependent variable (e.g., transport distance of tracers) or a binary dependent variable (e.g., entrainment or deposition of tracers). This approach was implemented as it can account for the characteristics of a given population (e.g., weight, size, location of tracers in channel, etc...) and determine if their levels of influence on sediment transport are significant. Furthermore, interactions between variables and their level of significance can also be determined.

Investigating the influence that large wood has on tracer entrainment, deposition, and transport distances required an analysis of all the potential variables that influence transport behaviour, as well as producing a testable variable for the influence of wood. The distance of tracer sediments to large wood in both their deposition and entrainment positions was determined in ArcGIS 10.6.1 using the Near (Analysis) proximity toolset, by mapping all mobile tracers to their nearest piece of large wood using their GPS locations for each annual dataset. This generated an inventory of spatial data that was used to determine the relative influence of distance to wood on sediment transport. Other key variables considered and determined were distance to channel thalweg (calculated using the same approach of distance to wood), distance to boulders and non-wood steps, and tracer sediment size (represented by b-axis length). The influence of differing river discharge year on year was not included directly in the LMM analysis, with each year being considered separately to isolate the effect of variables such as wood from annual changes in hydrology. Analysis of yearly LMM results is subsequently discussed in the context of associated flow rates, estimates of stream power, and degree to which critical thresholds are exceeded.

The relative influence of other geomorphic features, including the spatial location of boulders and non-wood steps, were found to not be significant using LMM analysis and therefore were not included in subsequent analysis. Insignificant LMM results are available in supplementary information (S3).

To isolate the influence of large wood pieces and remove anthropogenic bias from initial ‘hypermobility’ seen in previous tracer studies (e.g., Bradley and Tucker, 2012), tracers were selected for LMM analysis if their deposition location was downstream from the seeded reach after each year of the study from 2017. This area of the reach was also selected due to the abundance of large wood providing greater interaction with transported sediments. Finally, wood pieces classified as bridges were not included in the LMM analysis due to their lack of interaction with the bed.

The lme4 package in R (Bates et al, 2015) was used for LMM analysis. We used a binomial LMM model to investigate the relative influence of variables on the likelihood of entrainment and deposition of tracer sediments, and a gamma model to investigate a given variable’s influence on tracer transport distance.

#### **4. Results**

The discharge data for 2017 – 2019 show peak flow to be occurring during the summer months of May, June, and July (figure 3). 2017 flow rates initially rise in late May from a base level of  $\sim 0.5 \text{ m}^3 \text{ s}^{-1}$  to peak conditions of  $1.4 - 2.2 \text{ m}^3 \text{ s}^{-1}$  over June followed by a continuous return to base flow during July. 2018 flow rates were consistently the lowest of the three years surveyed with flow rising from the base rate of  $\sim 0.5 \text{ m}^3 \text{ s}^{-1}$  in May to peak conditions ranging from  $1.1 - 1.6 \text{ m}^3 \text{ s}^{-1}$  over June before again dropping to base conditions. 2019 flow rates were substantially higher, with two distinctive periods of increasing and



lowering flow rates over June and July peaking at  $2.9 \text{ m}^3 \text{ s}^{-1}$ . The recurrence interval for the peak flow rates in 2019 at the analogous stream Bobtail Creek are 1.9 years, suggesting even our highest measured flow rates are relatively common.

Stream power at annual peak flow was calculated for the average channel width of 5.5 m and average channel slope of 0.046 and was found to be 180.5, 131.3, and  $237.93 \text{ W m}^{-2}$  for 2017, 2018, and 2019 respectively. Stream power exceeded the estimated critical threshold (Ferguson 2005) for the  $D_{50}$  of tracer sediments of  $83.93 \text{ W m}^{-2}$  in all years surveyed, where a discharge value exceeding  $1.02 \text{ m}^3 \text{ s}^{-1}$  was required to initiate movement. Thresholds were therefore exceeded for approximately 26, 24, and 45 days in 2017, 2018, 2019 respectively (figure 3). When subdividing the reach, the gentler sloping and wider seeded reach critical threshold ( $88.90 \text{ W m}^{-2}$ ) is still exceeded by estimated stream power in 2017 and 2019 ( $104.10 \text{ W m}^{-2}$  and  $137.22 \text{ W m}^{-2}$ ), although the 2018 stream power ( $75.70 \text{ W m}^{-2}$ ) is slightly lower than estimated the threshold. Despite this, tracers were still entrained and transported within the seeded reach, although at lower rates and subsequent transport distances than other survey years.

Discharge each year showed an expected correlation with the mean transport distance of tracer sediments and the likelihood of tracer movement (table 2), with 2019 and 2018 having the highest and lowest percentage of tracers transports respectively, and the highest and lowest maximum transport distances respectively. However, estimating the direct influence of flow rate on the likelihood of movement and distance moved is cautioned as retrieval rates differed between years, meaning the total population of tracer sediments is not accounted for. Furthermore, in 2017 sediments have the potential to be hypermobile as they were artificially placed on the bed surface without replacement of original sediments and are therefore not fully incorporated into the bed.

Observed changes to the overall geomorphology of the reaches are minimal over the 3 years of study. There was, however, an accumulation of sediments, including our tracers, around pieces of large wood (e.g., figure 1d) and some reworking of gravel bars observed. Wood transport was limited to only one tagged piece falling into the channel and moving downstream 25 m. No additional wood was recruited after the 2017 study year. This demonstrates that the majority of sediment-wood interaction over the three years of the study was related to immobile wood and therefore, wood classification had no observable impact on wood transport during our study.

Tracer retrieval rates were comparable to previous studies (Hassan and Bradley, 2017), between 75% in 2018 and 88% in 2017 (table 2). The tracer population has a grain size distribution range of 47 – 110 mm with a median b axis diameter of 73 mm, which is larger than the  $D_{50}$  (53 mm) of the bed surface material, giving the majority of tracer sediments a  $D_i / D_{50}$  of  $> 1$  relative to bed material.

Maximum tracer transport distances in 2017, 2018, and 2019 were 109, 58, and 133 m respectively, with one clast travelling a cumulative 193 m downstream over the study period (table 2). Of the 49% of cobbles that became mobile during our study 73% of these travelled beyond the seeded reach. The tracer transport distance probability density functions in 2017 and 2019 fit a gamma distribution, although the data from 2018 show a weaker gamma distribution fit that is interrupted between tracer transport distances of  $\sim 15 - 25$  m (figure 5). The associated power law exponent,  $\beta$ , is  $> 2$  for all three years, representing superdiffusive behaviour, although the 2018  $\beta$  value of 2.3 is close to the threshold of  $\beta = 2$  for this characterisation, matching with the interruption seen in the gamma distribution fit. This is suspected to be caused by a clustering of tracers around a piece of large wood (the fallen tree) that entered the seeded reach in 2017 (figure 6). This wood piece was initially transported downstream 20 m to its deposition location and was subsequently incorporated into the bed

with increasing burial occurring every year. The increased density of tracer deposition in close proximity to this wood piece gives an initial indication of the impact of large wood on bedload transport which is further investigated using LMM analysis.

## **4.2 Linear mixed modelling of influence of wood and other variables on tracer transport**

### **4.2.1 Probability of tracer entrainment**

Linear mixed modelling (LMM) provides a statistical assessment of the influence of large wood on sediment transport. LMM of sediment entrainment likelihood in relation to distance to wood of tracer entrainment location across all years is significant to at least a 99% level of confidence using the binomial modelling approach, with 2018 and 2019 reaching > 99.9% levels of confidence (table 3). This confirms that proximity to wood pieces has a significant influence on entrainment likelihood, where tracers closer to wood pieces are less likely to be entrained. Clasts residing at > 5 m from wood are 37.5% more likely to be entrained than those < 1 m on average over the study (figure 7).

The tracer b-axis and relative distance to channel thalweg were also investigated for their influence on entrainment likelihood. The influence of b-axis on entrainment likelihood was found to be significant in 2018 and 2019 with smaller tracers more likely to be entrained. Distance to channel thalweg was found to be significant in 2017 and 2019 with tracers closer to the channel thalweg more likely to be entrained. Clasts found at > 3 m from the thalweg are at least 55% and 27% less likely to move in 2017 and 2019 respectively (table 3, figure 7).

#### **4.2.2 Influence of entrainment location on tracer transport distance**

A first LMM gamma model investigated the relationship between entrainment location variables and subsequent tracer transport distances. The influence of proximity to wood on tracer transport distance is significant to at least a 95% level of confidence in each year, with 2017 and 2018 reaching 99.9% levels of confidence (table 4, figure 8). The closer a tracer is located to wood when it is entrained, the shorter its subsequent transport distance.

Unsurprisingly, shorter distances from the channel thalweg were also significant for longer rock transport distances in 2018 and 2019 with at least a 99% level of significance. The b-axis of tracers was significant every year to at least a 95% level of significance, where shorter b-axis size resulted in longer transport distances of tracers (table 4).

#### **4.2.3 Downstream factors influencing rock transport distance**

A final LMM gamma model investigated the relationships between location in which tracers were deposited and tracer transport distance prior to deposition. This analysis reveals a trapping influence of wood on sediment when comparing rock transport distance with depositional proximity to large wood, i.e. large wood is associated with a shortening in transport distance. This is significant in 2019 at a 95% level of significance (table 5, figure 9). The same relationship occurs in 2017 and 2018, though is not significant above a 95% level of confidence. Clasts deposited closest to the thalweg had the longest transport distances, with at least a 95% level of significance. Finally, the b-axis of tracers was significant every year to at least a 95% level of significance, with the largest clasts having shorter transport distances.

### **4.3 Making predictions of sediment transport from linear mixed models**

Figure 8 displays the positive relationship between increased tracer transport distance and greater distances of tracers entrainment positions from wood for all years based on the gamma LMM output. This approach can be used to estimate a tracer's transport distance based on its initial distance from large wood before entrainment. For instance, in 2019, a clast located approximately 5 m from a large wood piece will move downstream approximately 30 m streamwise on average, with transport distance increasing the further a tracer is entrained from large wood. Conversely, figure 8 displays the inverse relationship between increasing tracer transport distance and increased tracer distance from channel thalweg at entrainment position. Additionally, figure 7 displays the relatively negative correlation between the distance of the tracer from the thalweg and probability of entrainment. These models can both be used to estimate a tracer's transport distance and movement likelihood in relation to this variable. For example, a tracer 2 m from thalweg is predicted to have a transport distance of 6 m on average from its entrainment position.

While these estimations can give an approximate transport distance or probability of movement based on the single variable dataset, direct extrapolation from the graphs does not include the influence of other variables, limiting the applicability outside of the general correlation and relative influence of each variable. However, they do provide a clear indication that proximity to large wood, distance from channel thalweg, and sediments b-axis all play an influential role on transport behaviour.

## **5. Discussion**

### **5.1. Influence of wood on stochastic sediment transport dynamics**

Stochastic sediment transport dynamics may be described with a combination of tracer transport distances and rest time distributions. We were unable to return to the field site to resurvey in due to Covid 19 restrictions on travel for two years, hence are limited to 3 years of resurvey data of the planned 5. In addition, implementation of active tags with embedded accelerometers (Dost, 2020; Maniatis, 2020; Dini et al., 2021) was interrupted and therefore data was insufficient to build a distribution of particle rest times and thus fully characterize sediment transport behaviour. However, we have been able to build distributions of tracer transport distances for the three resurvey years and observe deviations in these distributions as a result of wood-loading.

Qualitatively, large wood appears to alter the spatial deposition of sediments. One example observed was a dead tree that fell from the bank during runoff in 2017, floated roughly 20 m and deposited in the downstream end of the seeded reach. Sediments were subsequently observed accumulating around the wood piece, with ramping of sediments up the root wad in 2018 (figure 1d) and progressively incorporating the wood further into the bed by 2019. Additionally, our RFID tracer sediments were deposited more densely in close proximity to the wood piece in 2018 and 2019 comparatively to the rest of the seeded reach (figure 6), which displays otherwise similar morphological characteristics. In addition, tracers were observed to accumulate in the pools of log steps (e.g., figure 1e), supporting Wohl and Scott's (2017) finding that rivers with wood see an increase in pool sediment volume, alongside accumulating behind log steps forming a ramp (e.g., figure 1f).

While the tracer transport distance probability density functions for 2017 and 2019 in figure 5 appear to match well with the overlain expected gamma distribution (Bradley and Tucker, 2012) and the associated exceedance probability displays the expected super diffusive behaviour (e.g.,  $\beta > 2$ ), the 2018 plot breaks from this trend, and its  $\beta$  value of 2.3 is closer to the super - sub diffusive threshold of  $\beta = 2$ . This change could suggest a quantifiable

influence of wood is observable, at least in 2018, where lower shear stress due to a more moderate flow year (figure 3) increases woods impact on tracer movement as the blocking effect is more difficult to overcome, although these changes could be attributed to alterations in the vertical mixing of sediments (Hassan *et al.*, 2013). While channel morphology's impact on transport distributions could offer another explanation (e.g., Pyrce and Ashmore, 2003), the visual and recorded observations of clustering sediments around the large wood piece located within the seeded reach (figure 5) supports wood as a particularly important factor for the disruption in transport distributions.

Whilst the influence of wood on the distribution of tracer transport distance is not definitive, LMM modelling helped to demonstrate the trapping influence of wood more clearly. LMM modelling in 2019 (table 5, figure 9) showed that tracers deposited closer to wood had shortened transport distances prior to being deposited, suggesting a trapping effect. The cause of trapping and reduced transport distances is likely related to wood loading increasing roughness within the fluvial system (Buffington and Montgomery, 1999). This agrees with other sediment transport investigations where roughness was found to be a key influencing factor on reducing transport distances of sediments (e.g., Roth *et al.*, 2020).

The lack of statistical significance for the influence of wood on shortening rock transport distances in 2017 and 2018 is potentially related to the lack of wood found in the areas 1 to 10 m downstream of the seeded reach (figure 1), where the majority of tracers were deposited during the first two years of the study. By 2019 the number of tracers deposited within the wooded reach is greatly increased, alongside more tracers interacting with wood throughout the length of the study area as seen in figure 1a. This resulted in a population of tracers large enough to demonstrate a significant interaction, and positive correlation (e.g., figure 9), between deposition location of tracers in relation to wood and transport distance of tracers.

Results from the binomial LMM analysis demonstrate how the presence of wood in St. Louis Creek is reducing entrainment likelihood of sediment (table 3, figure 7). Whilst this result is significant every year, there is a slight decrease in significance in 2019. We suspect that the higher proportion of tracer sediments moved in 2019, resulting from the higher flow rates and subsequent stream power, could lessen the impact wood has on entrainment, where higher shear stress from stronger flows negates the limiting effect wood has on sediment entrainment likelihood. In addition, many immobile clasts from previous years were entrained by reworking of the bed during higher flow rates, independent of the spatial location of wood pieces. Despite this, these results agree with the findings of previous studies that an abundance of wood caused fluvial systems to retain a greater proportion of sediment in storage in addition to reducing overall sediment transport rates (Buffington & Montgomery, 1999; Montgomery *et al.*, 2003; Wohl and Scott, 2017).

The LMM gamma model showed that the influence of distance to wood on subsequent tracer transport distance is significant for all years (table 4, figure 7), with a 99.9% degree of certainty in 2017 and 2018, dropping to 95% in 2019. This reduction in statistical significance is likely related to the proposed reduction of the influence of large wood in 2019 due to greater flow rates, where wood has reduced impact on tracers due to higher water levels causing tracers to more easily pass over wood pieces. Additionally, the accumulation of sediments ramping along the upstream side of pre-existing large wood could result in easier over passing of logs by 2019. Finally, it is possible for large wood to float during higher periods of runoff (Wohl and Scott, 2017), which may have allowed a larger proportion of particles to pass underneath in 2019.

Additional data would be needed to further assess the influence of wood on transport distance distributions, but this initial data indicates that wood is having a disruptive effect (figure 6).

The potential for prediction of sediment transport distance and likelihood shown in figure 8



and figure 9 is an example of how linear mixed modelling could be used to predict sediment transport in such settings. This study exemplifies how distances to wood from either depositional, or entrainment location can be used to predict sediment transport distances with a large enough population of tracers, while accounting for other influential variables such as distance to thalweg, and size of surveyed tracers.

## 5.2. Other controls on particle entrainment

Key variables identified to significantly influence particle entrainment with the binomial LMM approach included particle size (represented by b-axis in this study), agreeing with conventional understanding of the correlation between sediment size and entrainment likelihood (e.g., Ashworth and Ferguson, 1989), with smaller grain sizes having a greater probability of entrainment. This suggests, in our study area, that the role of protrusion on entrainment likelihood (e.g., Hodge *et al.*, 2020) is minimal, assuming that smaller grain sizes protrude less but yet were more likely to be entrained in our sample of pebble – cobble sized tracer sediments. Additionally, the distance of tracer sediments to channel thalweg has an influential role on entrainment likelihood, with sediments with closer proximity to channel thalweg having higher entrainment likelihood, due to increased shear in the thalweg (Petit *et al.*, 1987).

While b-axis size was found to be significant in influencing entrainment likelihood in 2018 and 2019, the results from the 2017 output were not significant (table 4). This is potentially related to the ‘hypermobility’ of sediments in the first year of the study, where sediments are not naturally incorporated into the channel bed (Bradley and Tucker, 2012). A caveat to b-axis tracer results would be that the  $D_{50}$  value of the tracer sediments (73mm) is larger than that of the bed material (53 mm), where the  $D_{50 \text{ tracer}} / D_{50 \text{ bed}} = 1.38$ , potentially making them unrepresentative of the total sediment population of the stream. The larger  $D_{50}$  of tracer

sediments were unavoidable due to the size of the embedded RFID tags requiring clasts large enough to drill. However, results likely well characterise the pebble – cobble proportion of sediments transport behaviour in gravel bed streams.

### **5.3. Limitations and future work**

While multiple researchers have used RFID technology in tagging coarse particle transport, there is a lack of a consistency in the methodologies applied (e.g., standard procedures for tagging and detection methods). This may lead to differences in retrieval rates and detection location accuracy due to experimental setup rather than environmental conditions. Therefore, future research should follow a standardised approach in RFID equipment used, depth of tag embedding, and tracer placement where possible to reduce operational interference.

Retrieval rates of tracers consistently stayed above 75% every year and even increased from 2018 to 2019, demonstrating the success and longevity of the approach even in complex environments such as wood loaded rivers. For instance, Liébault *et al.* (2012) and Olinde & Johnson's (2015) recovery rates decreased annually over their studies from 78%, 45%, 25% and 83%, 50% respectively, with burial being highlighted as a particular issue. This highlights the effectiveness of the RFID scanning technique implemented, as multiple tracers which were buried without visual confirmation were subsequently identified and located.

While these studies suggest a poor recovery rate, the technique is still relatively new, with developments in the technology ongoing. Cassel *et al.* (2017) used ultra-high frequency tags to overcome many of the limitations with traditional (low frequency) PIT tags, such as difficulties separating signals and short detection ranges (e.g., Lamarre *et al.*, 2005). This may allow tracer studies to occur in previously inaccessible environments, such as wide braided rivers.

Including stream power directly in the LMM analysis for individual clasts was beyond the scope of this study due to uncertainties in subdividing the reach into multiple distinct sections with justifiable stream power estimates. Only including clasts that have entered the wooded reach in the LMM accounts for the change in average slope and channel width between the two reaches, but future work would require more detailed measures of driving force to accurately assess forces acting on individual clasts. Despite this, we were still able to determine the influence of large wood on tracer transport probably because the critical stream power threshold was exceeded throughout the study reach and any relatively small changes in stream power between clasts within the wooded reach were unable to mask the impact of wood on sediment transport dynamics.

## **6. Conclusion**

We conducted a RFID tracer study in a wood-loaded, alpine stream in Colorado USA over three years to investigate the influence of large wood on stochastic sediment transport dynamics. We investigated the influence of wood on aspects of sediment transport including transport distance and entrainment probability and used the novel approach of linear mixed modelling to untangle the influence of wood from other controls and build predictive models of sediment transport. Over three years the tracer transport distance frequency distributions of tracers were found to match previous tracer research, with an expected gamma distribution and dispersion characteristics of sediments remaining superdiffusive as indicated by a power law exponent on the tail of the distribution,  $\beta > 2$  (e.g., Bradley and Tucker, 2012). However, flattening of the power law tail of the transport distance distribution in 2018 (figure 6), is suspected to result from the interception of tracers by a large wood piece during the lower

flows bringing it closer to more subdiffusive behaviour, i.e. with a  $\beta < 2$ . The LMM results support this clustering effect finding that large wood traps sediments and forces premature deposition and shorter transport distances. Furthermore, tracers with a closer proximity to large wood have a significantly reduced likelihood of entrainment, in addition to smaller transport distances, in comparison to tracers entrained from wood free areas. Meanwhile as expected, LMM also found that both rock transport distance and entrainment likelihood both decrease with increasing distance of tracers from the channel thalweg. Additionally, LMM found that smaller b-axis resulted in greater likelihood of entrainment and subsequent transport distances. These results indicate that streams undergoing increased wood loading would experience a significant reduction in entrainment and subsequent transport distances of cobble – pebble sized clasts in alpine environments.

The approaches implemented in this research can help inform future river management schemes by providing a methodology to determine the effectiveness, and potential side effects, of introducing engineered large wood structures (e.g., log jams) for natural flood management on sediment transport. Collection of additional data sets with different volumes and configurations of large wood under a broader range of grainsize and discharge regimes are necessary to determine if the observations reported in this paper are consistent and would allow further understanding of grain-scale bedload transport behaviour in wooded reaches.

## 7. References

Ashworth, P.J., Ferguson, R.I. (1989) Size-selective entrainment of bed load in gravel bed streams. *Water resources Research*. 25(4), 627-634.

Ancey, C., Davison, A., Bohm, T., Jodeau, M., Frey, P. (2008) Entrainment and motion of coarse particles in a shallow water stream down a steep slope, *Journal of Fluid Mechanics*., 595, 83–114.

Ancey, C., Bohorquez, P., Bardou, E. (2014) Sediment Transport in Mountain Rivers, *ERCOFTAC Bulletin*, 100, 37-52.

Ancey, C. & Bohorquez, P. (2018) Stochastic streams bedload transport in mountain, *E3S Web of Conferences*, 40, 05046.

Arnaud, F., Piégay, H., Vaudor, L., Bultingaire, L. and Fantino, G., 2015. Technical specifications of low-frequency radio identification bedload tracking from field experiments: Differences in antennas, tags and operators. *Geomorphology*, 238, 37-46.

Bates, D., Mächler, M., Bolker, B., & Walker, S. (2015). Fitting Linear Mixed-Effects Models Using lme4. *Journal of Statistical Software*, 67(1). doi:10.18637/jss.v067.i01

Bendix J. and Cowell, M. (2010) Fire, floods and woody debris: Interactions between biotic and geomorphic processes, *Geomorphology*, 116(3-4), 297-304.

Bradley, N. & Tucker, G. (2012) Measuring gravel transport and dispersion in a mountain river using passive radio tracers, *Earth Surface Processes and Landforms*, 37(10), 1034-1045.

Bradley, N. (2017) Direct Observation of Heavy-Tailed Storage Times of Bed Load Tracer Particles Causing Anomalous Superdiffusion, *Geophysical Research Letters*, 44(24), 12,227-12,235.

Bennett, S. J., Ghaneeizad, S. M., Gallisdorfer, M. S., Cai, D., Atkinson, J. F., Simon, A., Langendon, E. J. (2015) Flow, turbulence, and drag associated with engineered log jams in a fixed-bed experimental channel, *Geomorphology*, 248 1, 172-184.

Buffington, J. M., Montgomery, D. R. (1999) Effects of sediment supply on surface textures of gravel-bed rivers, *Water Resources Research*, 35, 3523 – 3530.

Cassel, M., Piégay, H., Fantino, G., Lejot, J., Bultingaire, L., Michel, K., Perret, F. (2020) Comparison of ground-based and UAV a-UHF artificial tracer mobility monitoring methods on a braided river, *Earth Surface Processes and Landforms*, 45, 1123 – 1140.

Chapuis, M., Bright, C.J., Hufnagel, J. and MacVicar, B., 2014. Detection ranges and uncertainty of passive Radio Frequency Identification (RFID) transponders for sediment tracking in gravel rivers and coastal environments. *Earth Surface Processes and Landforms*, 39(15), 2109-2120.

Clauset, A., Shalizi, C., Newman, M.E.J. (2009) Power-law distributions in empirical data, *SIAM Review*, 51(4), 661-703.

Dhont, B., and Ancey, C. (2018) Are Bedload Transport Pulses in Gravel Bed Rivers Created by Bar Migration or Sediment Waves?. *Geophysical Research Letters*. 45(11). 5501-5508.

Dini, B., Bennett, G., Franco, A., Whitworth, M., Cook, K., Senn, A., Reynolds, J., (2021) Development of smart boulders to monitor *mass movements via the Internet of Things: A pilot study in Nepal*, *Earth Surface Dynamics*, *Earth Surface Dynamics*, 9, 295–315, <https://doi.org/10.5194/esurf-9-295-2021>

Dost, B., Gronz, O., Casper, M., Krein, A. (2020) The Potential of Smartstone Probes in Landslide Experiments: How to Read Motion Data. *Natural Hazards and Earth System Sciences*. 20, 3501–3519, <https://doi.org/10.5194/nhess-20-3501-2020>.

Dunnink, J., Hartley, R., Rutina, L., Alves, J., & Franco, A. (2019) A socio-ecological landscape analysis of human–wildlife conflict in northern Botswana. *Oryx*, 1-9. doi:10.1017/S0030605318001394

East, A.E., Pess, G.R., Bountry, J.A., Magirl, C.S., Ritchie, A.C., Logan, J.B., Randle, T.J., Mastin, M.C., Minear, J.T., Duda, J.J., Liermann, M.C., McHenry, M.L., Beechie, T.J., Shafroth, P.B. (2015) Large-scale dam removal on the Elwha River, Washington, USA: River channel and floodplain geomorphic change. *Geomorphology* 228, 765–786.

Ferguson, R. & Wathen, S. (1998) Tracer-pebble movement along a concave river profile: virtual velocity in relation to grain size and shear stress. *Water Resources Research*, 34, 2031–2038.

Ferguson, R.I., (2005). Estimating critical stream power for bedload transport calculations in gravel-bed rivers. *Geomorphology*, 70(1-2), 33-41.

Ferguson, R., Church, M., Rennie, C., Venditti, G. (2015) Reconstructing a sediment pulse: Modeling the effect of placer mining on Fraser River, Canada. *Journal of Geophysical Research: Earth Surface*, 120, 1436–1454.

Floyd, R.E. (2015) RFID in Animal-Tracking Applications, *IEEE*, 5, 32-33.

Gaeuman, D., Stewart, R., Schmandt, B., Pryor, C. (2017) Geomorphic Response to Gravel Augmentation and High-Flow Dam Release in the Trinity River. *Earth Surface Processes and Landforms*. 42(15), 2523–2540.

Golly A., Turowski J.M., Badoux A., Hovius N. (2019) Testing models of step formation against observations of channel steps in a steep mountain stream, *Earth Surface Processes and Landforms*, 44, 1390-1406.

Gippel C.J., O'Neill I.C., Finlayson B.L., Schnatz I. (1996) Hydraulic guidelines for the re-introduction and management of large woody debris in lowland rivers, *Regulated Rivers: Research & Management*, 12, 223–236.



Grabowski, R., Gurnell, A., Burgess-gamble, L., England, J., Holland, D., Klaar, M., Morrissey, I., Uttley, C., Wharton, G. (2019) The current state of the use of large wood in river restoration and management. *Water and Environment Journal*. 33(3), 366-377.

Green, G.N. (1992) The Digital Geologic Map of Colorado in ARC/INFO Format. Open-File Report 92-0507, U.S. Geol Sur, Denver, CO. available on-line (04/08/2020): <http://pubs.usgs.gov/of/1992/ofr-92-0507/>.

Gronz, O., Hiller, H., Wirtz, S., Becker, K., Iserloh, T., Seeger, M., Brings, C., Aberle, J., Casper, M., Ries, J. (2016) Smartstones: A small 9-axis sensor implanted in stones to track their movements. *CATENA* 142, 245-251.

Habersack, H. (2001) Radio-tracking gravel particles in a large braided river in New Zealand: a field test of the stochastic theory of bed load transport proposed by Einstein. *Hydrological Processes* 15, 377–391.

Hassan, M.A., Church, M. & Schick, A.P. (1991) Distance of movement of coarse particles in gravel bed streams. *Water Resources Research*, 27, 503–511.

Hassan, M.A. & Ergenzinger, P. (2003) Use of tracers in fluvial geomorphology. In *Tools in Fluvial Geomorphology*, Kondolf GM, Piégay H (eds). John Wiley & Sons: Chichester, 397–423.

Hassan, M.A., Voepel, H., Schumer, R., Parker, G., Fraccarollo, L. (2013) Displacement characteristics of coarse fluvial bed sediment. *Journal of Geophysical Research: Earth Surface*, 118, 155-165.

Hassan, M. A. and D. N. Bradley (2017). Geomorphic controls on tracer particle dispersion in gravel-bed rivers. *Gravel-Bed Rivers: Process and Disasters*: 159-184.

Helley, E. J., & Smith, W. (1971) Development and Calibration of a Pressure-Difference Bedload Sampler. Open-File, USGS, *Water Resources Division*, Menlo Park, California.

Hodge, R., Voepel, H., Leyland, J., Sear, D., Ahmed, S. (2020) X-ray computed tomography reveals that grain protrusion controls critical shear stress for entrainment of fluvial gravels, *Geology*, 48(2): 149–153.

Hubbell, D. W. (1964) Apparatus and Techniques for Measuring Bedload. U.S. Geological Survey, *Water Supply Paper*, 1748.

Keller, E.A. (1970) Bedload movement experiments, Dry Creek, California. *Journal of Sedimentary Petrology*, 40, 1339-1344.

Kelsey, H, Lamberson R, Madej M. (1987) Stochastic model for the long- term transport of stored sediment in a river channel. *Water Resources Research*. 23. 1738–1750.

Kinzel, P. (2009) *Channel Morphology and Bed Sediment Characteristics Before and After Habitat Enhancement Activities in the Uridil Property, Platte River, Nebraska, Water Years 2005–2008*, USGS Open-File Report 2009–1147.

Klaar, M.J., Hill, D.F., Maddock, I., Milner, A.M. (2011) Interactions between instream wood and hydrogeomorphic development within recently deglaciated streams in Glacier Bay National Park, Alaska. *Geomorphology* 130, 208–220.

Lane, P. and Sheridan, G. (2002) Impact of an unsealed forest road stream crossing: waterquality and sediment sources. *Hydrological Processes*. 16, 2599 –2612.

Langford T., Langford J., Hawkins S. (2012) Conflicting effects of woody debris on stream fish populations: implications for management. *Freshwater Biology*, 57, 1096–1111.

Lamarre, H., MacVicar, B. and Roy, A.G., 2005. Using passive integrated transponder (PIT) tags to investigate sediment transport in gravel-bed rivers. *Journal of Sedimentary Research*, 75(4), 736-741.

Laronne, J. & Carson, M. (1976) Interrelationships between bed morphology and bed-material transport for a small, gravel-bed channel. *Sedimentology*, 23, 67–85.

Legleiter, J.C. & Kyriakidis, P.C. (2006) Forward and Inverse Transformations between Cartesian and Channel-fitted Coordinate Systems for Meandering Rivers, *Mathematical Geology*, 38(8), 927-958.

Liébault, F., Bellot, H., Chapuis, M., Klotz, S., Deschâtres, M. (2011) Bedload tracing in a high-sediment-load mountain stream. *Earth Surface Processes and Landforms*. 37 (4), 385-399.

MacVicar, B. J. and Papangelakis, E., (2022) Lost and found: Maximizing the information from a series of bedload tracer surveys. *Earth Surface Processes and Landforms*, 47(2), 399-408.

Malmon, D. V., Dunne, T., & Reneau, S. (2003) Stochastic theory of particle trajectories through alluvial valley floors. *The Journal of Geology*, 111(5), 525–542.

Malmon D. V. (2005) Influence of sediment storage on downstream delivery of contaminated sediment. *Water Resources Research*. 41.

Maniatis, G., Hoey, T., Hodge, H., Rickenmann, D., Badoux, A. (2020) Inertial drag and lift forces for coarse grains on rough alluvial beds measured using in-grain accelerometers. *Earth Surface Dynamics*. 8, 1067–1099.

Martin, R. L ., Jerolmack, D. J., Schumer, R. (2012) The physical basis for anomalous diffusion in bed load transport. *Journal of Geophysical Research Earth Surface*. 117.

McDermott Long, O., Warren, R., Price, J., Brereton, T.M., Botham, M.S. and Franco, A.M., (2017) Sensitivity of UK butterflies to local climatic extremes: which life stages are most at risk?. *Journal of Animal Ecology*, 86(1), 108-116.

McNamara, J.P., Borden, C. (2004) Observations on the movement of coarse gravel using implanted motion-sensing radio transmitters. *Hydrological Processes* 18, 1871–1884.

Montgomery, D., Collins, B., Buffington, J., Abbe, T. (2003) Geomorphic effects of wood in rivers. *The Ecology and Management of Wood in World Rivers, Symposium*. 37, 21-47.

Nichols, M. H., (2004) A radio frequency identification system for monitoring coarse sediment particle displacement. *Applied Engineering Agriculture* 20, 783–787.

Nikora, V., H. Habersack, T. Huber and I. McEwan (2002). "On bed particle diffusion in gravel bed flows under weak bed load transport." *Water Resources Research* 38(6): 17-11-17-19.

Olinde, L. & Johnson, J. (2015) Using RFID and accelerometer-embedded tracers to measure probabilities of bed load transport, step lengths, and rest times in a mountain stream, *Water Resources Research*, 51, 7572-7589.

Oregon RFID, 2021, “Oregon RFID: Fish and Wildlife Tracking PIT Tags”

<https://www.oregonrfid.com/products/hdx-long-range-readers/mobile-reader-kit/>

Petit, F. (1987) The relationship between shear stress and the shaping of the bed of a pebble-loaded river (La Rulles-Ardenne). *Catena* 14(5), 453-468.

Petit, F., Gob, F., Houbrechts, G. and Assani, A.A., 2005. Critical specific stream power in gravel-bed rivers. *Geomorphology*, 69(1-4), 92-101.

Pickup, G., Higgins, R., Grant I. (1983) Modelling sediment transport as a moving wave — The transfer and deposition of mining waste. *Journal of Hydrology*. 60(1–4), 281-301.

Powell, J.A., Logan, J.A. (2005) Insect seasonality: circle map analysis of temperature-driven life cycles. *Theoretical Population Biology*, 67, 161–179.

Pyrce, R. S. and P. E. Ashmore (2003). "Particle path length distributions in meandering gravel-bed streams: Results from physical models." *Earth Surface Processes and Landforms* 28(9): 951-966.

Raffa, K.F, Aukema, B.H, Bentz, B.J, Carroll, A.L, Hicke, J. A, Turner, M.G, Romme, W.H. (2008) Cross-scale Drivers of Natural Disturbances Prone to Anthropogenic Amplification: The Dynamics of Bark Beetle Eruptions, *BioScience*, 56(6), 501-517.

Reneau, S. L., Drakos, P. G., Katzman, D., Malmon, D. V., McDonald, E. V., & Rytí, R. T. (2004) Geomorphic controls on contaminant distribution along an ephemeral stream. *Earth Surface Processes and Landforms*, 29, 1209–1223.

Roth, D. L., Doane, T. H., Roering, J. J., Furbish, D. J. and Zettler-Mann, A. (2020). Particle motion on burned and vegetated hillslopes. *PNAS*. 117(41). 25335-25343.

Ryan, S., Bishop, E.L., Daniels, J.M. (2014) Influence of large wood on channel morphology and sediment storage in headwater mountain streams, Fraser Experimental Forest, Colorado, *Geomorphology*, 217, 73-88.

Schenk, E. R., Moulin, B., Hupp C. R. Richte, J.M. (2013) Large wood budget and transport dynamics on a large river using radio telemetry, *Earth Surface Processes and Landforms*. 39 (4), 487-498.

Steeb, N., Rickenmann, D., Badoux, A., Rickli, C. and Waldner, P., 2017. Large wood recruitment processes and transported volumes in Swiss mountain streams during the extreme flood of August 2005. *Geomorphology*, 279, 112-127.

Slater, L. J., Singer, M. B., Kirchner, J. W. (2015) Hydrologic versus geomorphic drivers of trends in flood hazard. *Geophysical Research Letters*, 42, 370-376.

Sutherland, D., Ball, M., Hilton, S., Lisle, T. (2002) Evolution of a landslide-induced sediment wave in the Navarro River, California. *Geological Society of America Bulletin*, 114(8), 1036–1048.

Umazano, A., Melchor, R. (2020) Volcaniclastic sedimentation influenced by logjam breakups? An example from the Blanco River, Chile. *Journal of South American Earth Sciences*. 98.

Weeks, E., Swinney, H. (1998) Anomalous diffusion resulting from strongly asymmetric random walks. *Physical Review E*, 57(5), 4915–4920.

Wohl, E., Cenderelli, D.A., Dwire, K.A., Ryan-Burkett, S.E., Young, M.K., Fausch, K.D. (2010) Large in-stream wood studies: a call for common metrics. *Earth Surface Processes and Landforms*. 35, 618–625.

Wohl, E., Scott, D. (2017). Wood and sediment storage and dynamics in river corridors. *Earth Surface Processes and Landforms*. 42, 5-23.



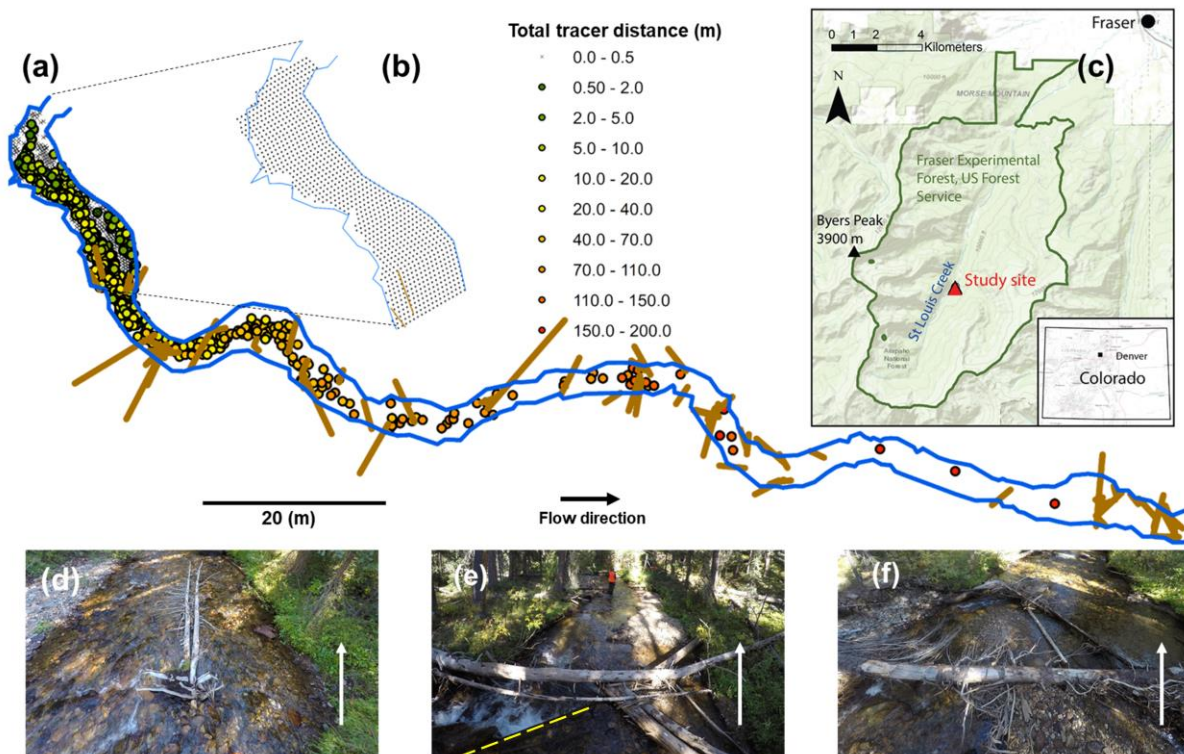


Figure 1: Overview of St. Louis creek with: (a) ArcMap spatial representation of study site with final (2019) locations of tracer sediments, with colour representing cumulative total tracer transport distance since the study began demonstrated by total cobble distance moved, and the location of large wood pieces that are interacting with bedload transport; (b) original seed locations of tracer sediments in 2016, known as the “seeded reach” (seed locations appearing to overlapping channel bank are a result of bank overhang); (c) location of study site within the Fraser Experimental Forest; (d) image representing area within seeded reach, which includes a wood piece that fell into the stream between 2016 and 2017; (e) buried wood (dashed yellow line) forming a log step and log jam approximately 100 m downstream of seeded reach; (f) a build-up of sediments behind large wood located just beyond the final tracer position. (Flow direction is approximately north in figure c and is represented by the white arrows on images).

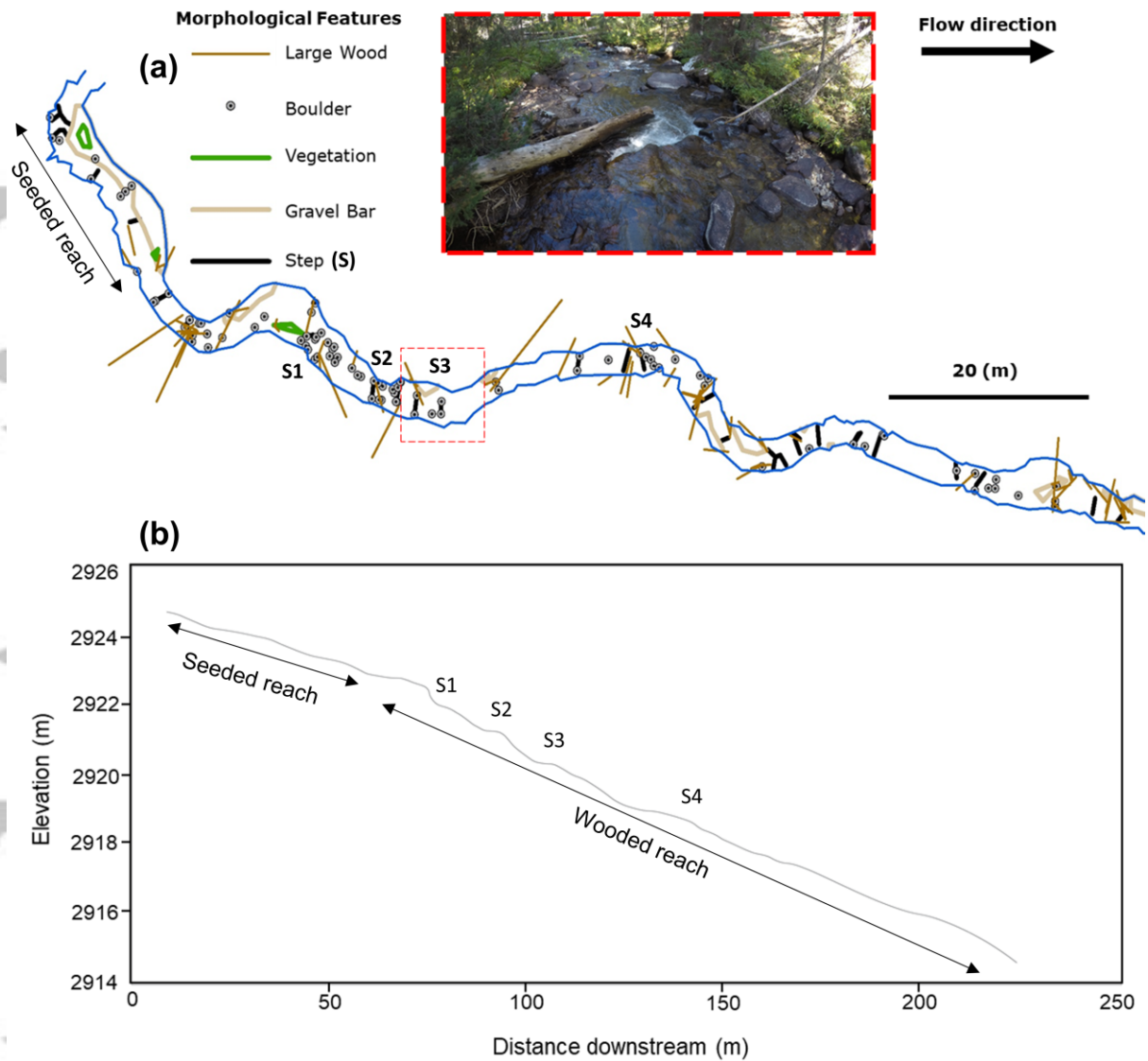


Figure 2: (a) morphological features surveyed at St. Louis creek including large wood, boulders, vegetation, gravel bars, and locations of steps. Area highlighted in dashed line as an image displays a typical section of the study area beyond the seeded reach with an example of a typical boulder step and large wood piece observable. (b) longitudinal profile of reach derived from tracer cobble elevations, with steps of interest labelled on feature map and profile (e.g., S1). Note the change to a steeper gradient slope from the end of the seeded reach into the wooded reach with the seeded and wooded reach having slopes of 0.0328 and 0.0502 respectively.

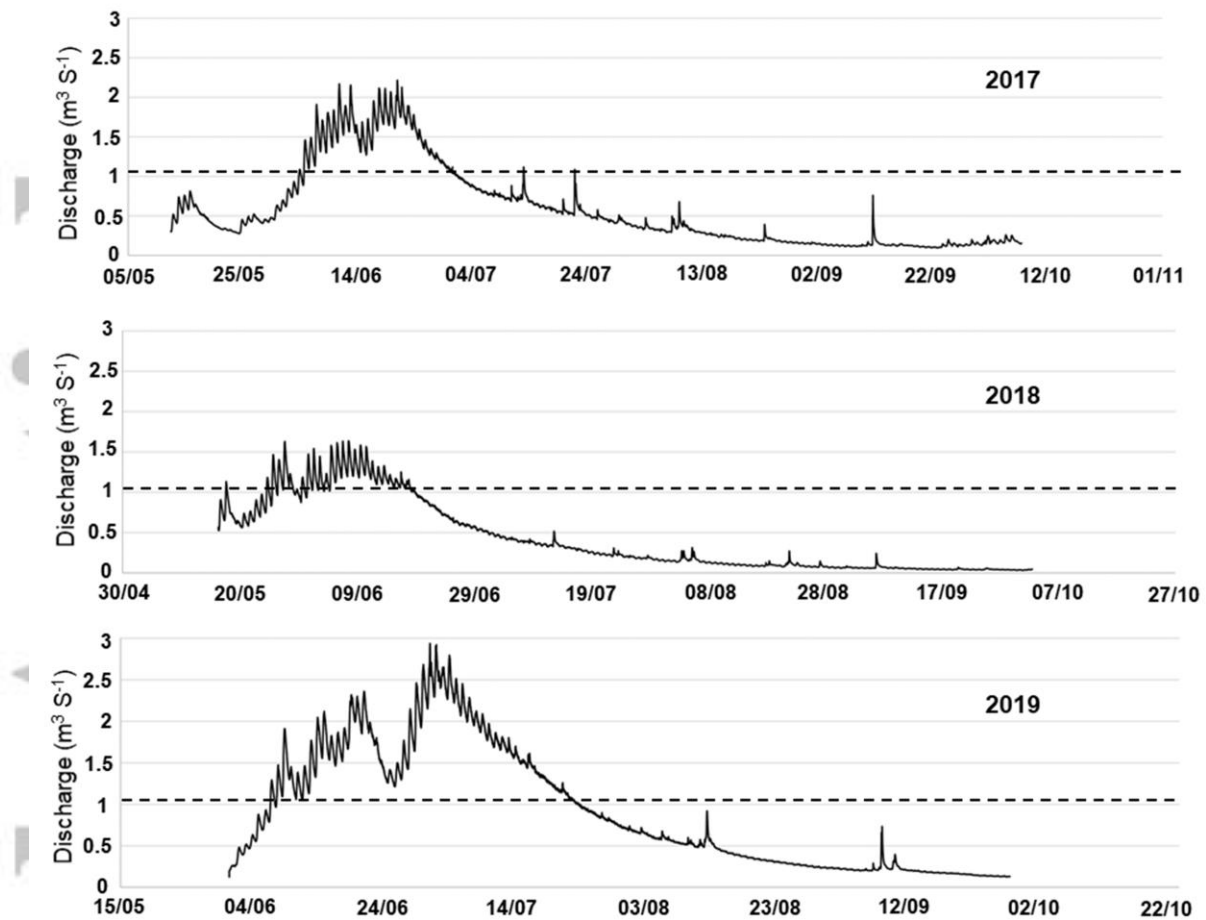


Figure 3: Annual discharge data from St. Louis Creek for 2017 – 2019 during periods of discharge gauge deployment upstream of study reach. Dashed line represents calculated discharge value of  $1.02 \text{ m}^3 \text{ s}^{-1}$  required to exceed estimated critical threshold (Ferguson 2005).

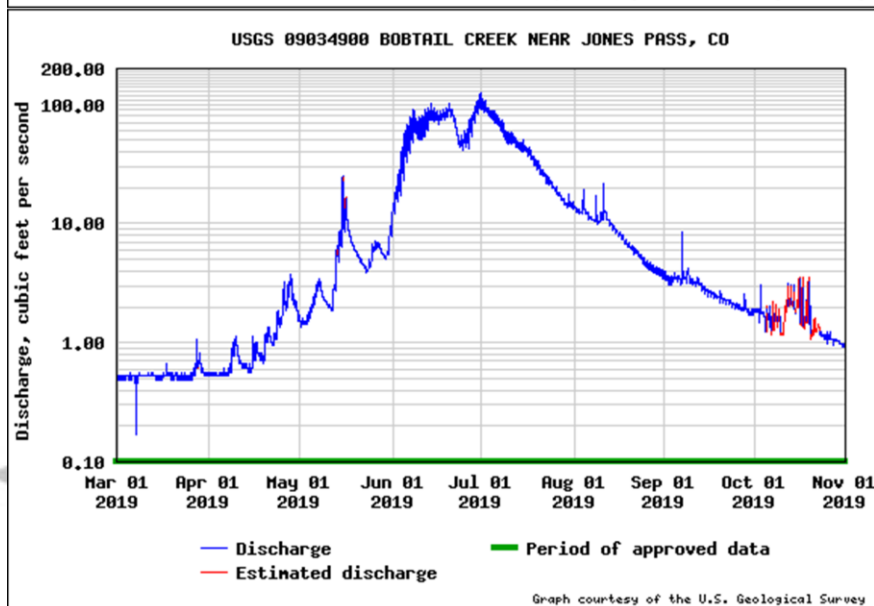
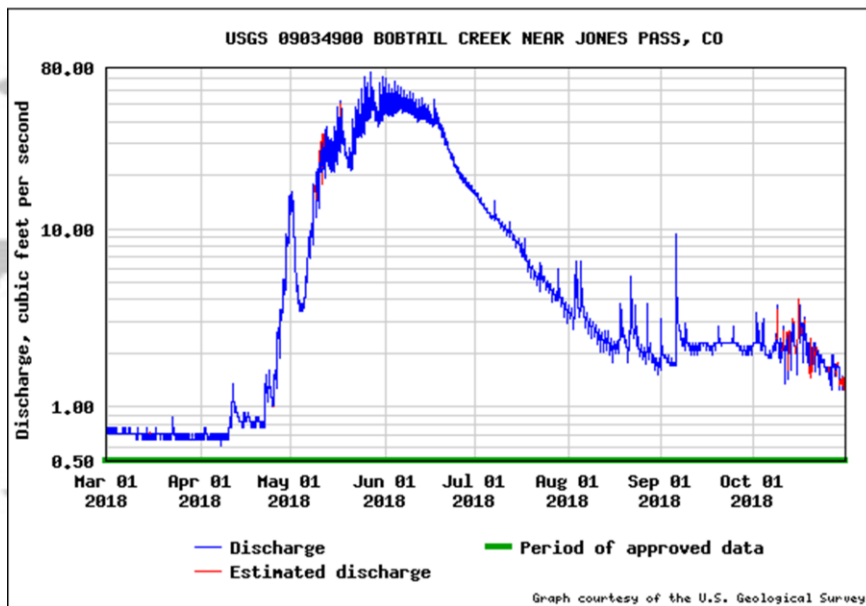
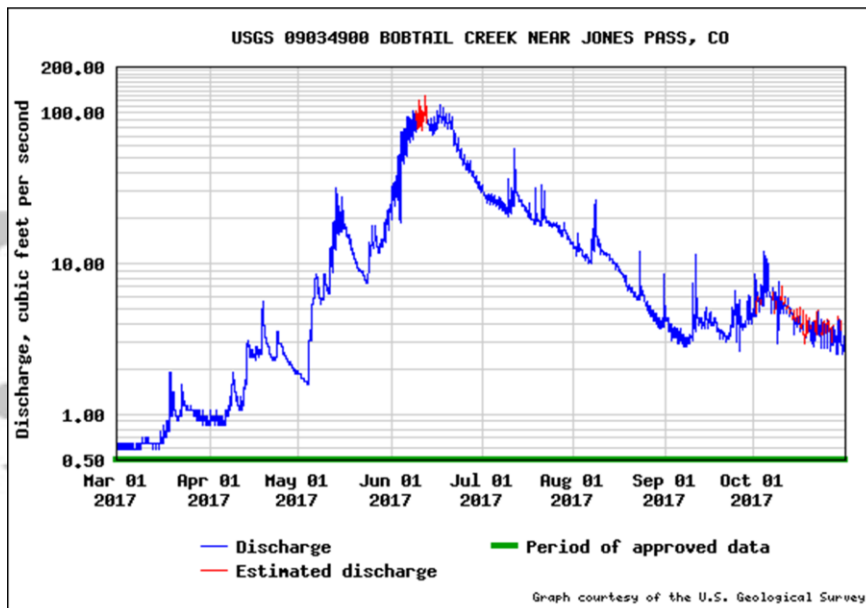


Figure 4: Discharge data from Bobtail Creek site for 2017 – 2019, demonstrating peak flow during summer after snowmelt matching with St. Louis Creek peak flow occurrence in figure 3. Analogous site chosen due to proximity, similar forest cover, and altitude to study site (USGS).

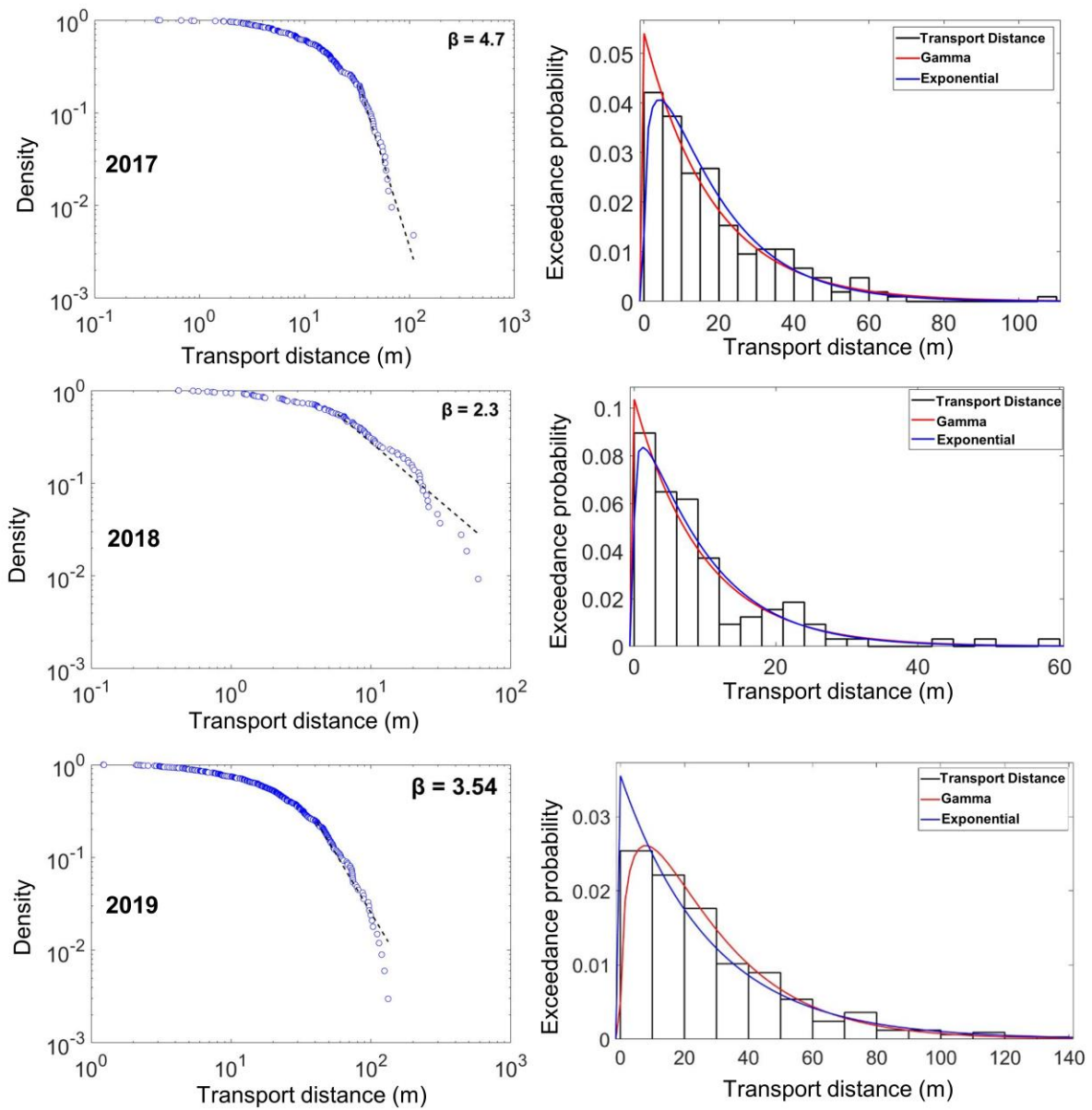


Figure 5: Tracer transport distance probability density functions with overlain exponential (Blue) and gamma (Red) curves alongside their annually associated exceedance probability graph with the power law fitting exponent line and  $\beta$  value representing the tail character of the data.



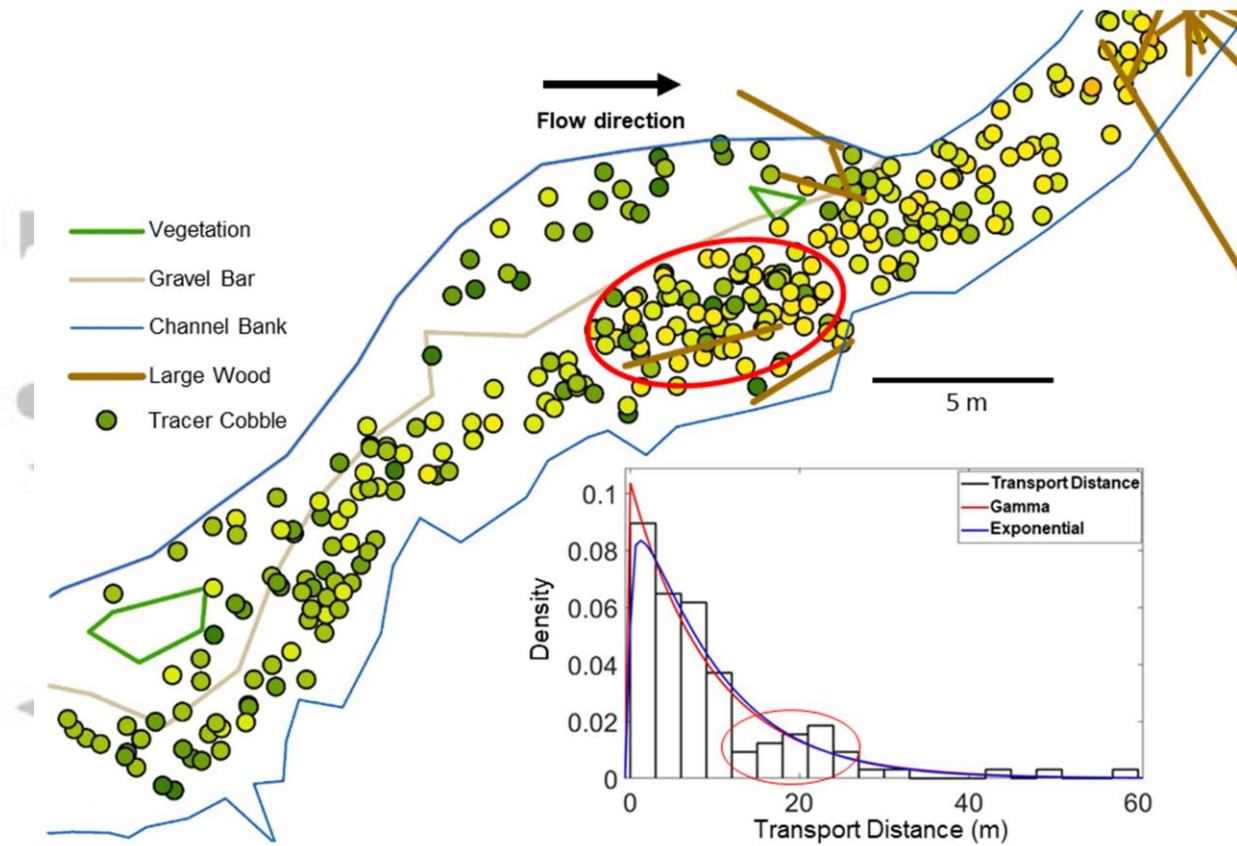


Figure 6: Observed clustering of tracer sediments from the 2018 data around the large wood piece located within the seeded reach (as seen in figure 1d). Note that the reversal of the trend in the probability density function in 2018 of figure 5 appears to match location of large wood piece (e.g., 15-25 m).

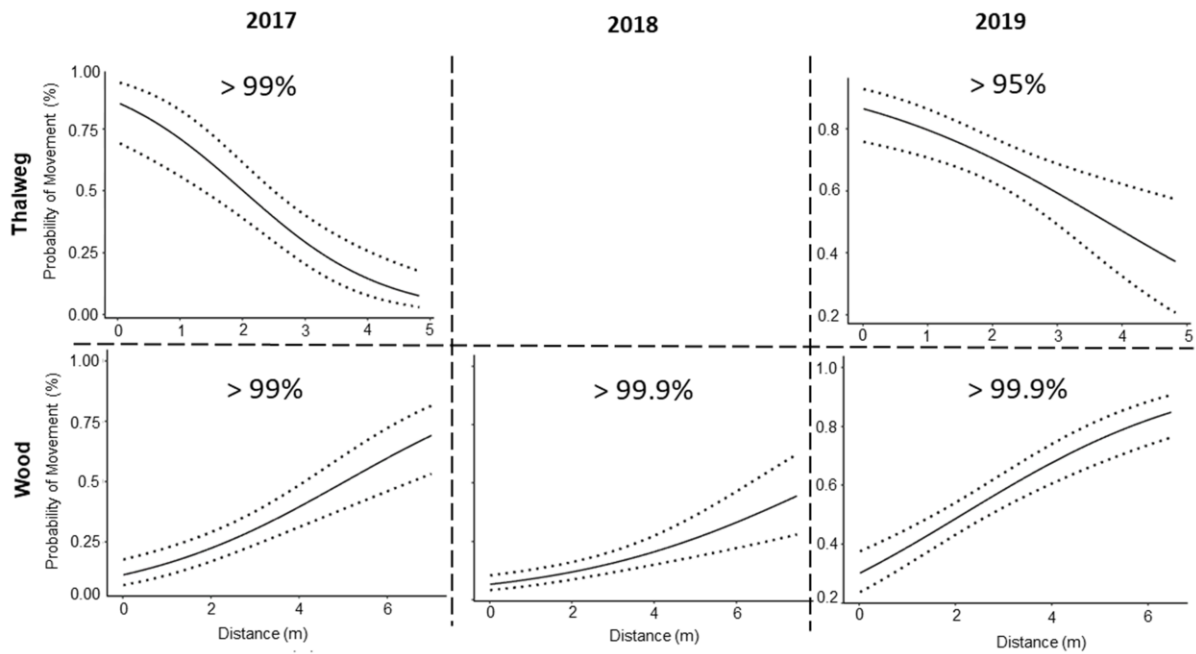


Figure 7: Relative influence of distance to thalweg at point of tracer entrainment (top), and distance to wood at point of tracer entrainment (bottom) on probability of tracer movement each year based on the binomial LMM prediction frame, with upper and lower bounds represented by dotted lines. Significant ( $> 95\%$ ) relationships between probability of movement and wood distances, or probability of movement and thalweg distances are plotted. Relationships below a 95% level of confidence are omitted (e.g., 2018 thalweg).



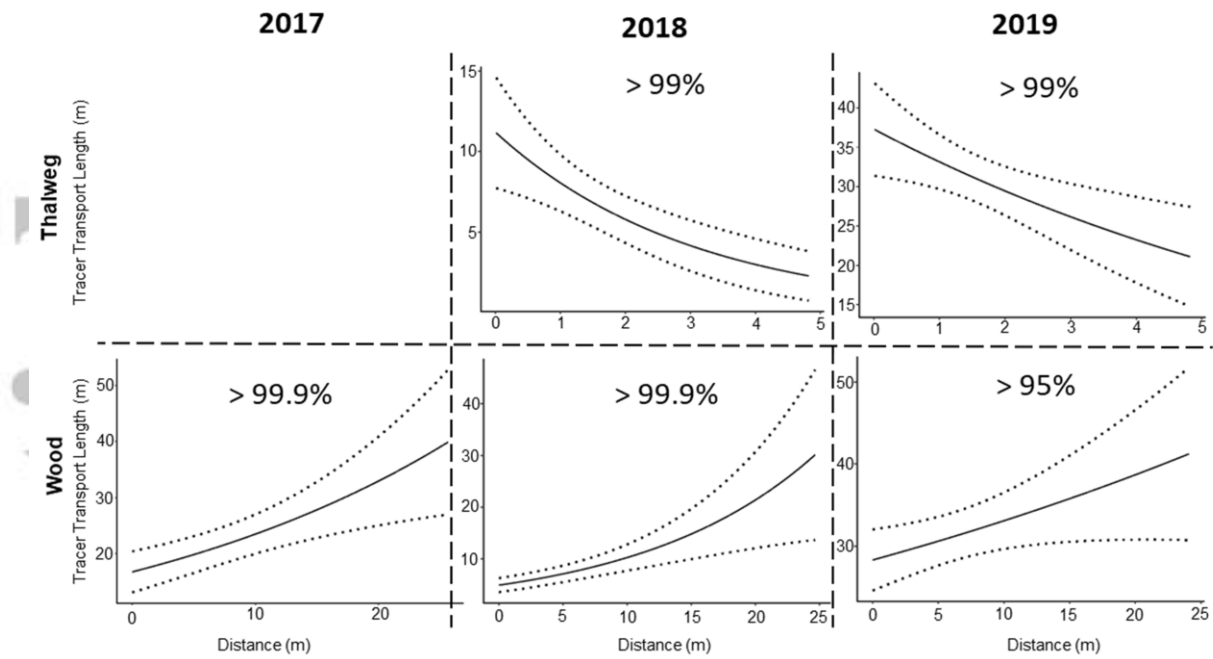


Figure 8: Relative influence of distance to thalweg at point of tracer entrainment (top), and distance to wood at point of tracer entrainment (bottom) on tracer transport length each year based on the gamma LMM prediction frame, with upper and lower bounds represented by dotted lines. Significant ( $> 95\%$ ) years relationships between tracer transport length and wood distances, or tracer transport length and thalweg distances are plotted, whilst relationship below a 95% level of confidence are omitted (e.g., 2017 thalweg).

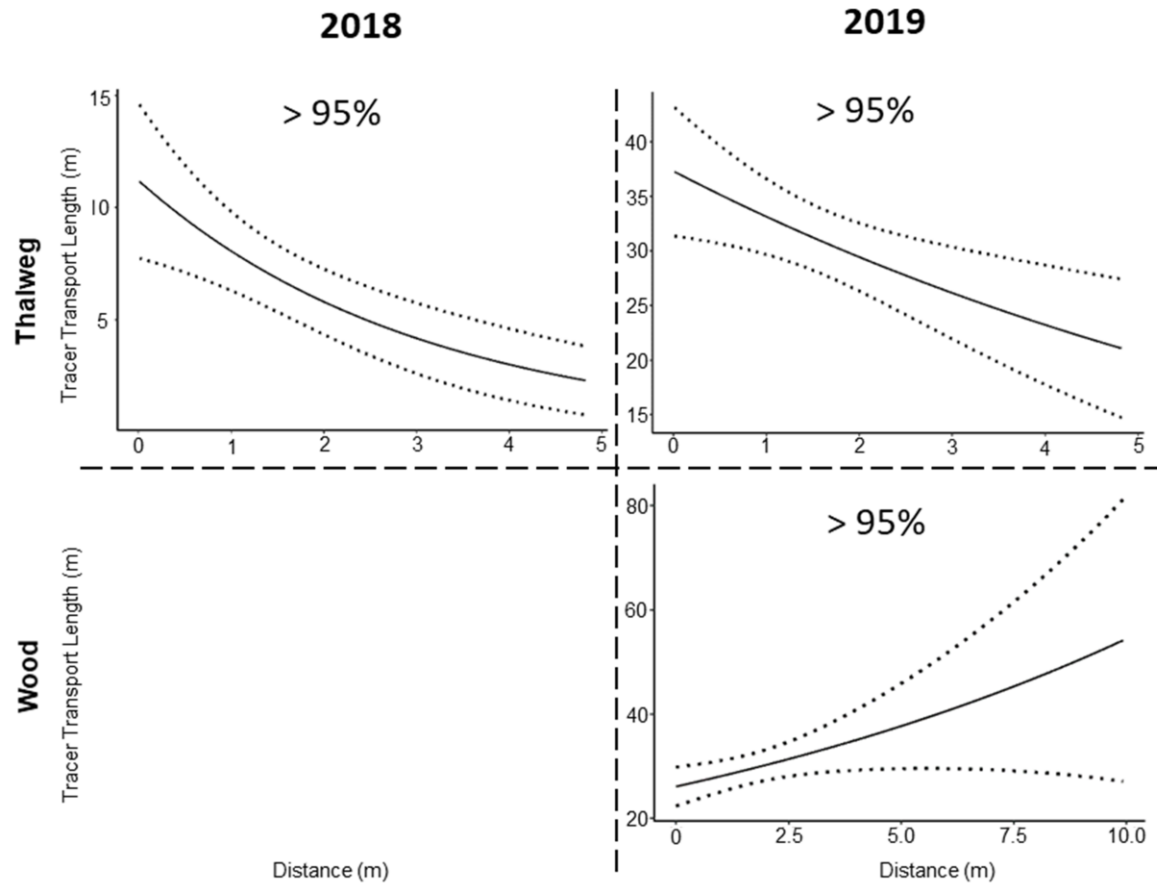


Figure 9: Relative influence of distance to thalweg upon tracer deposition (top), and distance to wood upon tracer deposition (bottom) on tracer transport length each year based on the gamma LMM prediction frame, with upper and lower bounds represented by dotted lines. Significant (> 95%) years relationships between tracer transport length and wood distances, or tracer transport length and thalweg distances are plotted, whilst relationship below a 95% level of confidence are omitted (e.g., insignificant relationships in 2017).

*Table 1: Key size and weight statistics of sediments selected for RFID tagging*

	Weight (g)	B - axis (mm)
Mean	636.1	74.2
Median (range)	605.5 (201.1 - 1483.3)	74.0 (47.0 - 110.0)
Mode	465.7	78
Standard deviation ( $\sigma$ )	208.7	10.3

Table 2 Key statistics of tracer sediment movement, showing annual and cumulative results of transported sediments

Year	Retrieval Rates (%)	Cobbles Moved (%)	Median B-Axis and range (m)	Maximum Tracer Transport Distance (m)	Peak river discharge ( $\text{m}^3 \text{s}^{-1}$ )	Mean Tracer Transport Distance (m)
2017	88	22	73 (50 – 110)	109	2.217	29.96
2018	75	11	73 (51 – 110)	58	1.634	9.63
2019	80	35	73 (48 – 102)	133	2.938	28.14
<b>Total</b>	<b>81*</b>	<b>49</b>	N/A	<b>193</b>	N/A	

\* = Mean retrieval rates

*Table 3: Linear mixed model output data for the likelihood of tracer sediment entrainment within the wooded reach, including the coefficient, standard error, z-value and p-value for all variables. P values indicated with a \*, \*\*, and \*\*\* represent a 95%, 99%, and 99.9% level of confidence respectively.*

<b>2017 Binomial</b>	<b>Coefficient</b>	<b>Standard Error</b>	<b>Z</b>	<b>P</b>
Distance to thalweg	-0.574	0.221	-2.603	0.0093**
Distance to wood	0.533	0.163	3.261	0.0111**
B – Axis	-0.015	0.015	-0.954	0.3398
<b>2018 Binomial</b>				
Distance to thalweg	-0.056	0.233	-0.240	0.81019
Distance to wood	0.664	0.155	4.293	<0.001***
B – Axis	-0.034	0.017	-2.012	0.0442*
<b>2019 Binomial</b>				
Distance to thalweg	-0.321	0.144	-2.227	0.026*
Distance to wood	0.458	0.012	3.950	<0.001***
B – Axis	-0.035	0.011	-3.313	0.0017**

Table 4: Linear mixed model output data for the influence of distance to wood, thalweg, and b-axis on the transport distance of tracer sediments at the point of entrainment within the wooded reach, including the coefficient, standard error, z-value and p-value for all variables. P values indicated with a \*, \*\*, and \*\*\* represent a 95%, 99%, and 99.9% level of confidence respectively.

<b>2017</b> <b>Entrainment</b>	<b>Coefficient</b>	<b>Standard Error</b>	<b>Z</b>	<b>P</b>
Distance to thalweg	-0.100	0.058	-1.721	0.00878
Distance to wood	0.034	0.008	3.799	0.0002***
B – Axis	-0.019	0.007	-2.890	0.0046**
<b>2018</b> <b>Entrainment</b>				
Distance to thalweg	-0.323	0.091	-3.633	<0.001***
Distance to wood	0.074	0.014	5.387	<0.001***
B – Axis	-0.020	0.009	-2.132	0.0369*
<b>2019</b> <b>Entrainment</b>				
Distance to thalweg	-0.118	0.044	-2.720	0.0067**
Distance to wood	0.016	0.007	2.241	0.0258*
B – Axis	-0.021	0.004	-4.686	<0.001***

Table 5: Linear mixed model output data for the influence of distance to wood, thalweg, and b-axis on the transport distance of tracer sediments at the point of deposition within the wooded reach, including the coefficient, standard error, z-value and p-value for all variables. P values indicated with a \*, \*\*, and \*\*\* represent a 95%, 99%, and 99.9% level of confidence respectively.

<b>2017 Deposition</b>	<b>Coefficient</b>	<b>Standard Error</b>	<b>Z</b>	<b>P</b>
Distance to thalweg	-0.112	0.066	-1.752	0.0823
Distance to wood	-0.115	0.059	-1.936	0.0552
B – Axis	-0.018	0.007	-2.723	0.0074**
<b>2018 Deposition</b>				
Distance to thalweg	-0.220	0.105	-2.105	0.039*
Distance to wood	-0.130	0.104	-1.245	0.2177
B – Axis	-0.023	0.011	-2.013	0.0485*
<b>2019 Deposition</b>				
Distance to thalweg	-0.191	0.052	-3.690	<0.001***
Distance to wood	0.073	0.031	2.400	0.017*
B – Axis	-0.002	0.004	-4.149	<0.001***

## Graphical abstract

Sediment transport distances displayed expected gamma distributions with sediment transport characteristics remaining superdiffusive, although clustering around large wood temporarily flattened the power law tail of these distributions. LMM analysis found large wood traps sediments and forces premature deposition and shorter step lengths. Furthermore, tracers with a closer proximity to large wood have a significantly reduced likelihood of entrainment, in addition to smaller transport distances, in comparison to tracers entrained in wood free areas.

